Supplemental Materials and Methods

Microarray Acquisition

Kasumi-1 cells were transduced with validated human PLCG1 shRNAs or non-targeting control (n=4). 48 hours post-infection, puromycin was added to select for transduced cells. Three days post-infection total RNA of $2x10^6$ cells was isolated using the TRIzol-Chloroform method as described before [1]. RNA quality was assessed using the Agilent 2100 Bioanalyzer. Microarray analysis was performed by Arraystar Inc. (Rockland, MD, USA) using the Arraystar Human LncRNA Expression Array V4.0 (Agilent-079487) designed to interrogate human lncRNAs and coding genes. Briefly, rRNA was removed from 1µg of total RNA. Each sample was amplified and transcribed into fluorescent cRNA (Arraystar Flash RNA Labeling Kit) using a random-priming method, thus capturing the entire length transcripts without 3`bias. The labeled cRNA was hybridized onto the Arraystar Human LncRNA Micoarray V4.0. After washing the slides, the arrays were scanned by the Agilent DNA Microarray Scanner. Agilent Feature Extraction software (version 10.7.3.1) was used to analyze acquired array images.

Microarray annotation

Microarray data was analyzed by R 3.5.1 and Bioconductor 3.7 [2]. Since the annotation of noncoding RNAs in particular is subject to frequent changes we re-annotated all 60898 unique probes interrogating human transcripts on the Human LncRNA Array V4.0 platform by mapping the probes to the current release of the human transcriptome (Gencode Release 28, GRCh38.p12, April 2018). The FASTA files containing the sequences of all 203,835 human transcripts in the Gencode database were downloaded (ftp://ftp.ebi.ac.uk/pub/databases/gencode/Gencode_human/release_28/gencode.v28. transcripts.fa.gz) and each 60mer probe was aligned to the transcript collection allowing for 4 mismatches using the R package "Biostrings". For each matching transcript the ensembl gene ID was retrieved. The R package "biomaRt" [3] was used to retrieve further annotation such as the gene symbol and transcript type of each matching ensemble gene ID from Ensemble. This yielded 35,440 annotated probes. For probes without a match in Gencode we used the annotation supplied by the manufacturer. The remaining unannotated probes were aligned to the high confidence set of the lncipedia 5.2 database of noncoding transcripts

(https://lncipedia.org/_downloads/lncipedia_5_2.fasta) [4]. In total 47,665 probes interrogating 20822 protein coding transcripts and 26843 non-coding RNAs were annotated using this pipeline. The R script of the annotation pipeline is available upon request.

Microarray analysis

RAW files were read in using the function "read.maimages" from the R package "limma" [5]. Probe intensity distributions and PCA of the unprocessed RAW data were used to assess array quality. RAW data was quantile normalized and duplicate probes on the array were averaged using the functions "normalizeBetweenArrays" and "avereps" from "limma", respectively. For further computations the dataset was reduced to the 47,665 annotated probes. For principal components analysis we filtered the dataset for the top 5% of probes with the highest variation using the package "genefilter" followed by the function "prcomp" from the R package "stats". To compute differentially expressed genes the "limma" package was employed using a cutoff of Benjamini-Hochberg adjusted *p*-values < 0.05 and $\log_2 FC > 1$. For Gene Set Enrichment Analysis (GSEA) the expression matrix was filtered to contain only genes occurring at least once in the MSigDB GeneSet Database v6.2 [6]. In case a gene was interrogated by more than one probe, the probe with the higher variation was selected, resulting in an expression set of 17,847 probes with unique gene symbols. A preranked gene list was computed comprised of the $\log_2$ fold changes between knockdown and control samples for all 17,847 genes using the "limma" package. The gene list was submitted to the Broad GSEA tool using "GSEA-preranked" with the permutation type set to Gene_set (1,000 permutations). We tested a custom gene set collection comprised of 166 gene sets related to hematopoiesis and leukemia [7]. In addition, the C2, C5 and hallmark gene set collections from MSigDB.v6.2 (http://software.broadinstitute.org/gsea/downloads.jsp) comprised of 10840 gene sets were tested for enrichment. The enrichment results were either visualized by plotting the normalized enrichment score against the false discovery rate or by using the output from GSEA as input for the Enrichment Map Tool [8] for Cytoscape 3.6.1. Enrichment map was created with the following parameters: *FDR* <0.02, similarity coefficient between gene sets >0.4 and Jaccard Overlap Combined Index = 0.5. Red and blue nodes represent enrichment in the shPLCG1 and shCtrl groups, respectively. Clusters of nodes were labelled manually according the most often represented biological process contained in the respective clusters.

Analysis of DNaseI and ChIP-sequencing data

Published ChIP-sequencing data set GSE54478 [9], GSE121282 [10] and GSE117108 [11] was used for analysis. For analysis of the raw sequence reads in fastq format was aligned to the hg19 human genome build using Bowtie2 [12]. The quality control statistics for the samples were obtained using FastQC software (http://www.bioinformatics.babraham.ac.uk/projects/fastqc/). The reads uniquely aligned to chromosomal positions in bam format were retained and the duplicate reads were removed using Picard tools (http://broadinstitute.github.io/picard/). The filtered aligned reads were used to generate density maps using bed-tools [13] and data was displayed using the UCSC Genome Browser [14].

Regions of enrichment (peaks) of ChIP and DNAseI sequencing data were identified using MACS [15] and cisGenome [16] software. The resulting peaks common for the two peak calling methods were considered for further analysis. High confidence ChIP-Seq peaks were defined as those overlapping peaks in the DNaseI-seq data.

Proteome profiling by LC-MS/MS

For global proteome profiling, leukemia development was initiated with AE/K or MA9 containing MSCV-GFP constructs. Murine stem-and progenitor cells (LSK cells: Lin-Sca+Kit+) from 6-8 weeks-old C57BL/6J donors (females) were sorted and infected by co-localization of virus supernatant (containing one of the oncogenes) with LSK cells on retronectin-coated plates. 72 hours after infection equal numbers of GFP+ cells were injected into sublethally irradiated recipient hosts (7 Gy). $2x10^5$ LSC-enriched (GFP+Kit+) cells (4 replicates per oncogene) were sorted directly into 2x lysis buffer (for a final concentration: 1% SDS, 50 mM HEPES, pH 8.5, 10 mM DTT; volume of lysis buffer added to collection tube was estimated to be equal to the volume of the sheath buffer). For analysis of human samples, $2x10^5$ CD34+CD38+ cells from bone marrow aspirates from t(8;21)-positive (4 replicates) versus 4 t(8;21)-negative (4 replicates) AML patients were isolated by FACS sorting and applied to the proteomics pipeline. Samples were sonicated in a Bioruptor (Diagenode, Belgium) (10 cycles with 1 minute on and 30s off with high intensity at 20°C). Samples were then heated at 95°C for 10 minutes, before being subjected to another round of sonication. The lysates were cleared and debris precipitated

by centrifugation (14,000 rpm for 10 minutes), then incubated with 15 mM iodacetamide at room temperature 20 minutes. Each sample was treated with 8 volumes ice cold acetone and left overnight at -20°C to precipitate the proteins. The samples were then centrifuged at 14,000 rpm for 30 minutes at 4°C. After removal of the supernatant, the precipitates were washed twice with 500 µL of ice cold 80 % acetone. The pellets were then allowed to air-dry before being dissolved in digestion buffer (3M urea in 0.1 M HEPES, pH 8). To facilitate the resuspension of the protein pellet, the samples were subjected to 3 rounds of sonication in the Bioruptor, as described above. A 1:100 w/w amount of LysC (Wako sequencing grade) was added to each sample and samples were incubated for 4 h at 37 °C on a shaker. The samples were diluted 1:1 with milliQ water (to reach 1.5M urea) and were incubated with a 1:100 w/w amount of trypsin (Promega, Madison, WI, USA) overnight at 37 °C and 650 rpm. The digests were then acidified with 10% trifluoroacetic acid and desalted with *Waters Oasis® HLB µElution Plate 30µm* in the presence of a slow vacuum. In this process, the columns were conditioned with 3 x 100 µL solvent B (80% acetonitrile; 0.05% formic acid) and equilibrated with 3x100 µL solvent A (0.05% formic acid in milliQ water). The samples were washed 3 times with 100 µL solvent A, and then eluted into PCR tubes with 50 µL solvent B. The eluates were dried down with the speed vacuum centrifuge and dissolved in 5% acetonitrile with 0.1% formic acid to a final volume of 10 µL, which was transferred to an MS vial and 0.25 µL of HRM kit peptides (Biognosys, Zurich, Switzerland) was spiked into each sample prior to analysis by LC-MS/MS. For the sample pools, 2 µL of each sample contained within the pool was removed from the individual samples and 1.5 µL of this was injected for each of the DDA runs, in triplicate. 4.5 µL was injected per individual sample for DIA acquisition. Peptides were separated using the nanoAcquity UPLC MClass system (Waters) fitted with a trapping (nanoAcquity Symmetry C18, 5µm, 180 µm x 20 mm) and an analytical column (nanoAcquity BEH C18, 1.7µm, 75µm x 250mm). The outlet of the analytical column was coupled directly to Q-Exactive HFX (Thermo Fisher Scientific) using the Proxeon nanospray source. Solvent A was water, 0.1 % formic acid and solvent B was acetonitrile, 0.1 % formic acid. The samples (either a subset of the samples (mouse) or a pool of samples, injected in triplicate) were loaded with a constant flow of solvent A at 5 µL/min onto the trapping column. Trapping time was 6 min. Peptides were eluted via the analytical column with a constant flow of 0.3 µL/min. During the elution step, the percentage of solvent

B increased in a non-linear fashion from 0 % to 40 % in 60 min. Total runtime was 75 min, including clean-up and column re-equilibration. The peptides were introduced into the mass spectrometer via a Pico-Tip Emitter 360 µm OD x 20 µm ID; 10 µm tip (New Objective) and a spray voltage of 2.2 kV was applied. The capillary temperature was set at 300 °C. The RF ion funnel was set to 40%. Full scan MS spectra with mass range 350-1650 *m/z* were acquired in profile mode in the Orbitrap with resolution of 60000. The filling time was set at maximum of 20 ms with an AGC target of $1x10^6$ ions. The peptide match algorithm was set to "preferred" and only charge states from 2^+ to 5^+ were selected for fragmentation. The top 15 most intense ions from the full scan MS were selected for MS2, using quadrupole isolation and a window of 1.6 Da. An intensity threshold of $4 x10^4$ ions was applied. HCD was performed with normalized collision energy of 31%. A maximum fill time of 25 ms, with an AGC target of $2x10^5$ for each precursor ion was set. MS2 data were acquired in profile, with a resolution of 15000 with fixed first mass of 120 *m/z*. The dynamic exclusion list was with a maximum retention period of 30 sec and relative mass window of 10 ppm. Isotopes were also excluded. In order to improve the mass accuracy, internal lock mass correction using a background ion (*m/z* 445.12003) was applied. For data acquisition and processing of the raw data Xcalibur 4.0 (Thermo Scientific) and Tune version 2.9 were employed. Peptides were separated on the same LC gradient as for the DDA library creation. MS acquisition was performed with the same source settings as for DDA and the following method changes for the data acquisition. Full scan MS spectra with mass range 350-1650 *m/z* were acquired in profile mode in the Orbitrap with resolution of 120000. The default charge state was set to 3+. The filling time was set at maximum of 60 ms with limitation of $3x10^6$ ions. DIA scans were acquired with 22 (human samples) or 30 (mouse samples) mass window segments of differing widths across the MS1 mass range. HCD fragmentation (stepped normalized collision energy; 25.5, 27, 30%) was applied and MS/MS spectra were acquired with a resolution of 30000 with a fixed first mass of 200 *m/z* after accumulation of $3x10^6$ ions or after filling time of 47 ms (whichever occurred first). Data were acquired in profile mode.

MS raw data analysis

For library creation, the DDA and DIA data were searched independently using Pulsar in Spectronaut Professional+ (version 11.0.15038, Biognosys AG, Schlieren, Switzerland). The data were searched against a species specific (*Mus musculus* or *Homo sapiens*) Swissprot database. The data were searched with the following modifications: Carbamidomethyl (C) (Fixed) and Oxidation (M)/ Acetyl (Protein N-term) (Variable). A maximum of 2 missed cleavages for trypsin were allowed. The identifications were filtered to satisfy FDR of 1 % on peptide and protein level. For each species analysis, a DpD (DDA plus DIA) library was then created by merging the respective DDA and DIA libraries together in Spectronaut. These libraries contained 47291 (mouse); 45357 precursors, corresponding to 3781 (mouse); 3580 protein groups using Spectronaut protein inference. Relative quantification was performed in Spectronaut for each pairwise comparison using the replicate samples from each condition. The data (candidate table) and data reports (protein quantities) were then exported and further data analyses and visualization were performed with R-studio (version 0.99.902) (http://www.R-project.org/.) using in-house pipelines and scripts.

RNA-Sequencing Analysis

Sorted LSK cells from Plcg1F/F and Plcg1+/+ littermate controls were infected twice (8 hours gap) by spinfection with retroviral particles containing the AE9a/K oncogenes. $7.5x10^4$ GFP+ cells were injected into sublethally irradiated (7 Gy) primary recipient mice (C57BL/6J, female). GFP+Kit+ cells were isolated from leukemic mice and retrovirally transduced with a Cre-recombinase (MSCV-Cre-puro). 48 hours after infection puromycin (1µg/ml) was added for 24 hours. Cells were harvested and resuspended in TRIzol™, and RNA was extracted using the TRIzol-Chloroform method [1]. RNA-seq libraries were generated using SMART-Seq v4 Ultra Low Input RNA Kit (Takara Bio USA Inc., Mountain View, CA, USA) followed by Nextera XT (Illumina, San Diego, CA, USA).

For analysis, 50 bp single-end reads (Illumina) were aligned to reference genome mm10 and gtf.-transcriptome annotation release M7 (GENCODE) using STAR two-pass mode [17]. GENCODE M7 gtf.-file was used for quantification, performed by STAR, followed by normalization, transformation and

differential gene expression analysis in DEseq2 [18]. GSEA was carried out on a public server "Gene Pattern" of Broad Institute [19].

Supplemental Table 1. Flow cytometry and western blot antibodies used in this study.

Antibody	Source	Identifier
APC anti-mouse CD45.2	Biolegend	Cat #: 109814
APC anti-mouse Gr-1	Biolegend	Cat #: 108412
APC-Cy7 anti-mouse cKit	Biolegend	Cat #: 105826
APC-Cy7 anti-mouse CD11b	Biolegend	Cat #: 101225
APC-Cy7 anti-mouse CD3	Biolegend	Cat #: 100221
APC-Cy7 anti-mouse CD48	Biolegend	Cat #: 103431
AF 647 anti-mouse cKit	Biolegend	Cat #: 105818
BV 421 anti-Streptavidin	Biolegend	Cat #: 405226
FITC anti-mouse Sca-1	Biolegend	Cat #: 108106
FITC anti-mouse CD34	BD Biosciences	Cat #: 553733
Pacific Blue anti-mouse Gr-1	Biolegend	Cat #: 108430
PE anti-mouse CD45.1	Biolegend	Cat #: 110708
PE anti-mouse Gr-1	Biolegend	Cat #: 108408
PE-Cy7 anti-mouse F4/80	Biolegend	Cat #: 121114
PE-Cy7 anti-mouse CD19	Biolegend	Cat #: 115519
PE-Cy7 anti-mouse FcgR	Biolegend	Cat #: 101318
PE-Cy7 anti-mouse Ki-67	BD Biosciences	Cat #: 561283
PerCP-Cy5.5 anti-mouse Sca-1	Biolegend	Cat #: 108123
PerCP-Cy5.5 anti-mouse CD11b	Biolegend	Cat #: 101227
PerCP-Cy5.5 anti-mouse CD150	Biolegend	Cat #: 115921
Biotin anti-mouse CD3ε	Biolegend	Cat #: 100304
Biotin anti-mouse CD19	Biolegend	Cat #: 115503
Biotin anti-mouse Gr-1	Biolegend	Cat #: 108404
Biotin anti-mouse TER119	Biolegend	Cat #: 116204
Biotin anti-mouse B220	Biolegend	Cat #: 103203
Biotin anti-mouse CD4	Biolegend	Cat #: 100404
Biotin anti-mouse CD8	Biolegend	Cat #: 100704
Biotin anti-mouse IL7Ra	Biolegend	Cat #: 121104
Biotin anti-human CD45R/B220	Biolegend	Cat #: 103204
Biotin anti-human CD33	Biolegend	Cat #: 303426
Biotin anti-human CD235a	Biolegend	Cat #: 306618
Biotin anti-human CD3	Biolegend	Cat #: 344820
Biotin anti-human CD19	Biolegend	Cat #: 302204
Biotin anti-human CD14	Biolegend	Cat #: 367106
AF 647 anti-human CD45	Biolegend	Cat #: 304018
PE anti-human CD34	BD Biosciences	Cat #: 345802
PE-Cy7 anti-human CD13	BD Biosciences	Cat #: 338439
PE-Cy7 anti-human CD38	Biolegend	Cat #: 356607
anti-PLCG1 (1:1000)	Cell Signaling	Cat #: 2822
anti-ETO (1:1000)	Cell Signaling	Cat #: 4498
anti-CREB (1:1000)	Cell Signaling	Cat #: 9197
anti-JUN (1:1000)	Cell Signaling	Cat #: 9165
anti-FOS (1:1000)	Cell Signaling	Cat #: 4384
anti-GAPDH (1:5000)	Meridian Life Sciences	Cat #: H86504M

Supplemental Table 2. gRNA and shRNA sequences used in this study.

Gene	**Sequence (5`-3`)**
PLCG1 gRNA1-1	ATAGCGATCAAAGTCCCGTG
PLCG1 gRNA1-4	AGACCCCTTACGAGAGATCG
ETO gRNA	GGAAGAGGCGAACTCCAGAC
CREB1 gRNA#1	CAGCTGTACTAGAGTTACGG
CREB1 gRNA#2	TGGAGTTGGCACCGTTACAG
JUN gRNA#1	TCGTTCCTCCCGTCCGAGAG
JUN gRNA#2	GTCATGAACCACGTTAACAG
FOS gRNA#1	CTGCAGCCAAATGCCGCAAC
FOS gRNA#2	AGGTGACCACCGGAGTGCAC
RPA3 gRNA	GGTTGGAAGAGTAACCGCCA
Luc gRNA	GATTCTAAAACGGATTACCA
PLCG1 shRNA1-1	CCGGGCCATTGACATTCGTGAAATTCTCGAGAATTTCACG AATGTCAATGGCTTTTTG
PLCG1 shRNA1-2	GTACCGGAGAAGTTCCTTCAGTACAATCCTCGAGGATTGT ACTGAAGGAACTTCTTTTTTTG

Supplemental Table 3. Primer sequences for RT-qPCR and genotyping used in this study.

Gene	**Sequence (5`-3`)**
hu_B2M for	TGTGTCTGGGTTTCATCCATCCGA
hu_B2M rev	CACACGGCAGGCATACTCATCTTT
hu_PLCG1 for	AGTTCCTTCTTGACTACCAG
hu_PLCG1 rev	ACTCATCCAGGAAGAAGTATG
hu_GAPDH for	CCTGGCCAAGGTCATCCAT
hu_GAPDH rev	AGGGGCCATCCACAGTCTT
Plcg1_genotyping_for	ACCTCAGGCTCGTGTACG
Plcg1_genotyping_rev	CTAGGTCAGAGCAGGTCACT

Supplemental Figure 1

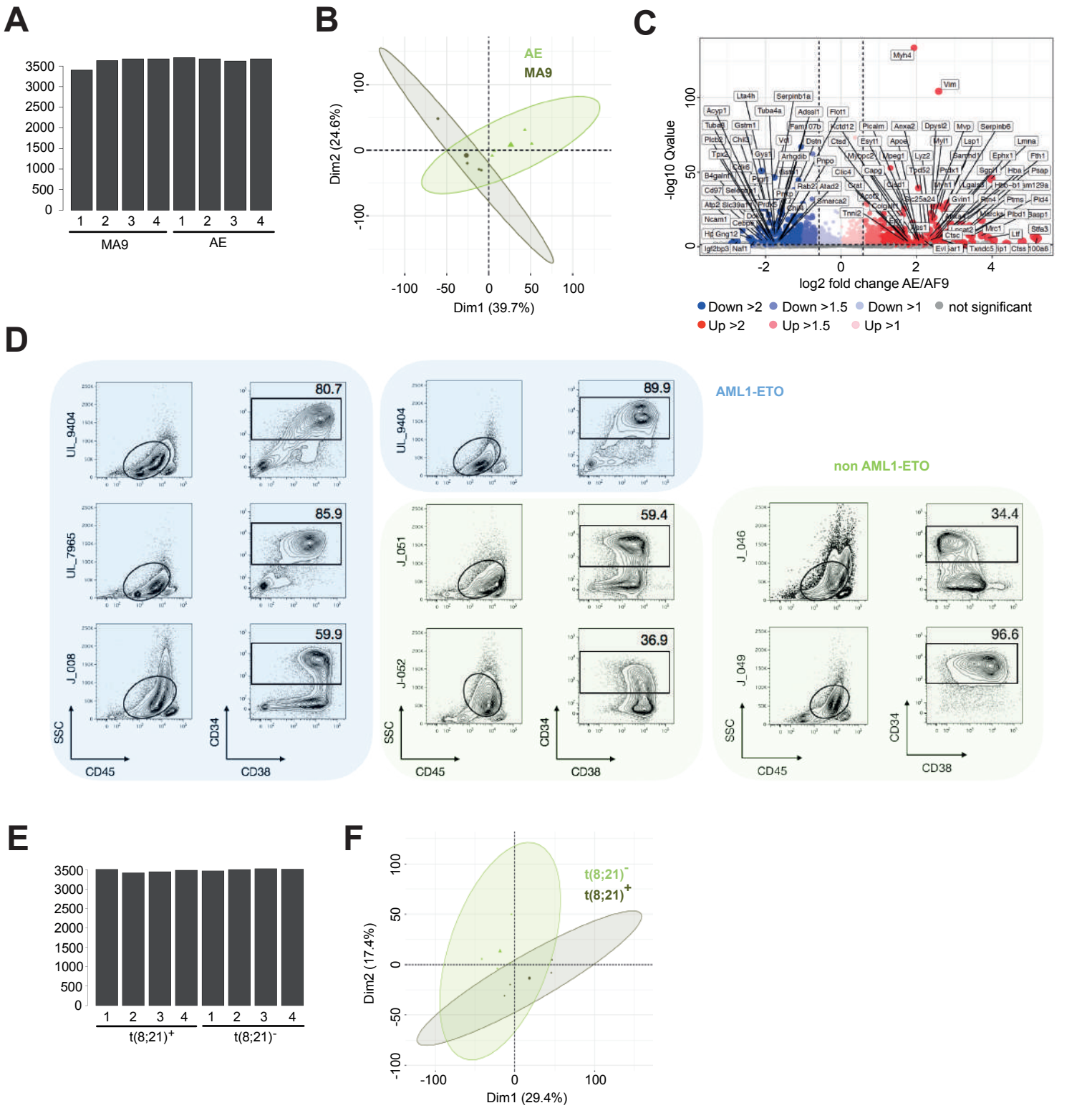

Supplemental Figure 1. Phospholipase C and Ca++ signaling is enriched in AML1-ETO transformed LSCs. (A) Bar chart of protein numbers detected per replicate for murine MLL-AF9 (MA9, *n*=4) and AML1-ETO9a (AE, *n*=4) LSC in mass spectrometry analysis. **(B)** Principal component analysis (PCA) on murine MA9 and AE LSC. **(C)** Volcano plot depicting all quantified proteins identified by mass spectrometry between AML1-ETO (AE) and MLL-AF9 (AF9) LSC-enriched populations. Four independent samples of each oncogene were analyzed. The *Q*-values (as –log10 values) were plotted against the log2 ratio of protein expression. The cutoffs for annotation were set to log2FC = ±1.58 (3-fold change), and –log10 (*Q*-value) ≥3 (*Q*-value ≤ 0.001) for ease of viewing the most significant differentially regulated candidates. **(D)** Flow cytometry plots displaying the sorting strategy of human CD34+CD38+ bone marrow cells from AML1-ETO-positive and AML1-ETO-negative (non AML1-ETO) patients analyzed by mass spectrometry (*n*=4 per genotype). **(E)** Bar chart of protein numbers detected by mass spectrometry per replicate for primary human CD34+CD38+ bone marrow cells from t(8;21)-positive and t(8;21)-negative AML patients. **(F)** Principal component analysis (PCA) on human CD34+CD38+ bone marrow cells from t(8;21)+ and t(8;21)- AML patients.

Supplemental Figure 2

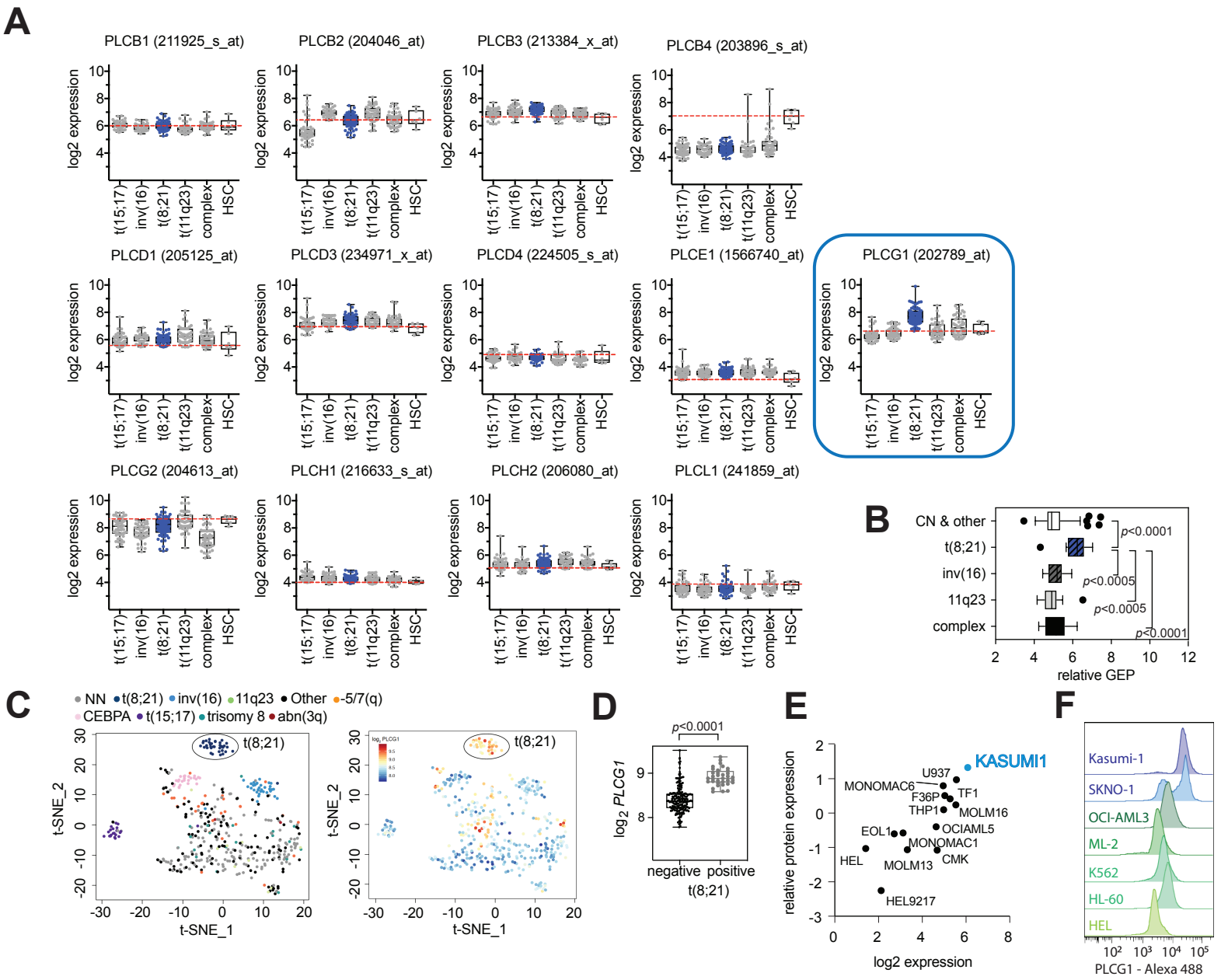

Supplemental Figure 2. *PLCG1* expression is highly increased in t(8;21) AML. (A) *In silico* analysis of PLC isoforms for mRNA expression in different subtypes of human AML (http://servers.binf.ku.dk/bloodspot/) reveals PLCG1 (blue box) to be highly expressed in primary t(8;21) AML. The data set used for analysis is mentioned in brackets. The red dotted line represents the mean expression in HSCs. **(B-D)** *In silico* analysis of PLCG1 mRNA expression in different subtypes of human AML. **(B)** GSE13204 (*n*=252) [20]; CN, cytogenetically normal, unpaired *t*-test. **(C)** t-SNE plot displaying the gene expression landscape of 457 AML patients from Wouters et al. [21] with an overlay of different AML subtypes (left) and with absolute PLCG1 expression values (right panel). **(D)** Scatterplot of PLCG1 expression of t(8;21)-positive (*n*=35) and –negative (*n*=422) AML patients (unpaired Welsh`s *t*-test) [22]. **(E)** Analysis displaying the gene expression (x-axis) and protein expression (y-axis) of PLCG1 in different AML cell line models (DepMap database, www.depmap.org). **(F)** Representative histogram showing PLCG1 protein expression in AML1-ETO positive (Kasumi-1, SKNO-1) versus AML1-ETO negative human AML cell lines analyzed by intracellular flow cytometry.

Supplemental Figure 3

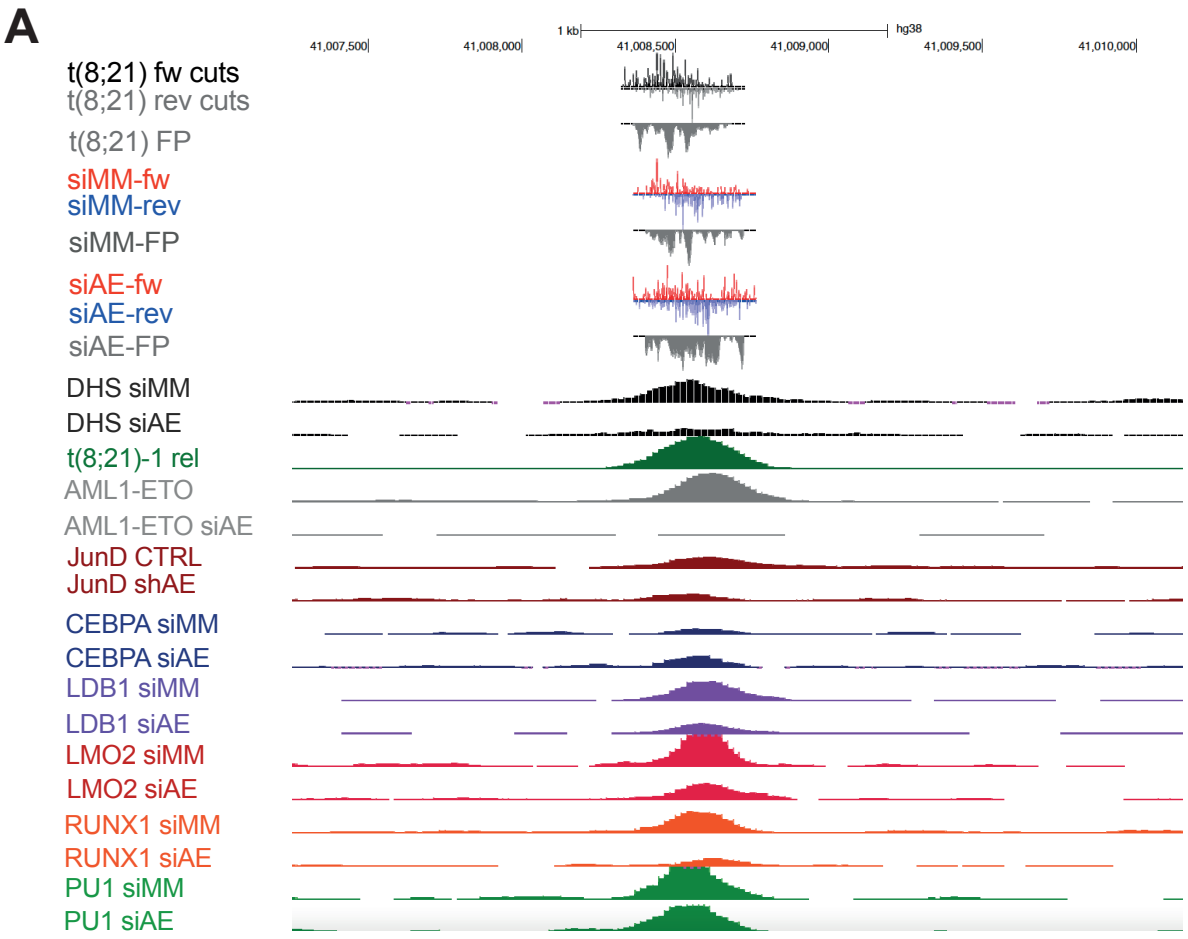

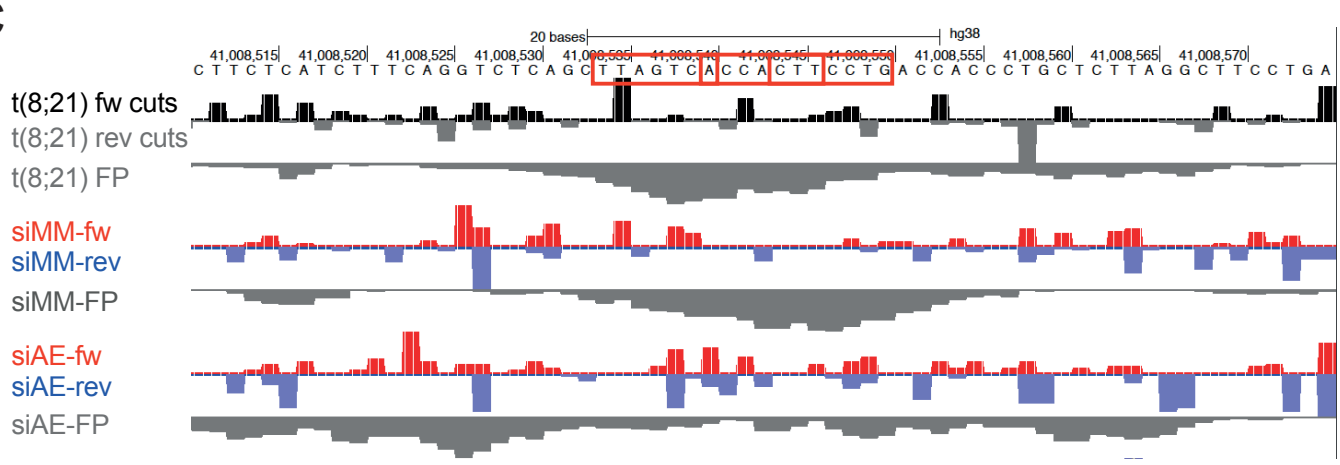

Supplemental Figure 3. High resolution depiction of the transcription factors binding to the -128 kb enhancer element in the presence or absence of AML1-ETO. (A) Zoomed in browser shot view of the DHSs and the transcription factors (AML1-ETO, JunD, CEBPA, LDB1, LMO2, RUNX1, PU.1) binding to the –128 kb enhancer with (siMM) or without (siAE) AML1-ETO knockdown. Top panel: DNaseI cuts on both DNA strands and digtal footprinting probabilities as identified by the Wellington [23]. Fw: forward strand, rev: reverse strand, FP: Footprint probability. **(B)** Sequence of the 500 bp enhancer element with the binding motifs for the indicated transcription factors highlighted in the sequence. The RUNX1 motif overlaps with an ETS motif forming a composite RUNX1-ETS site as described in Bevington et al. [24]. **(C)** Footprint probabilities at the sequence around the RUNX1 motif before and after AML1-ETO knockdown.

Supplemental Figure 4

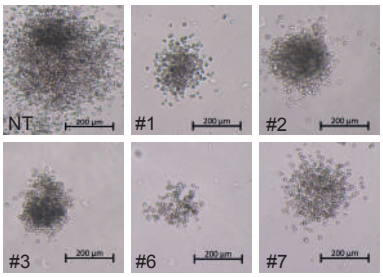

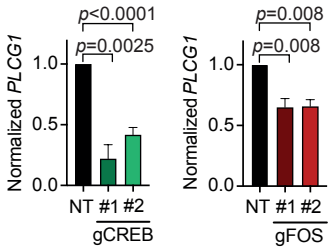

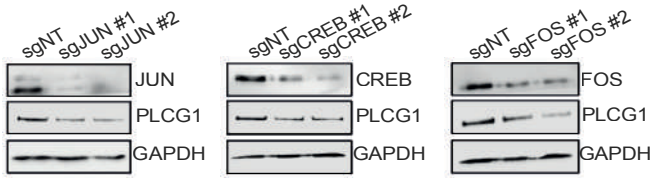

Supplemental Figure 4. An intergenic AML1-ETO binding non-coding element is essential for *PLCG1* expression. (A) Representative pictures of colonies of Kasumi_Cas9-EGFP cells following CRISPR/Cas9-induced knockout of the 500 bp intergenic region using specific gRNAs or a non-targeting control (NT) (day 14); scale bars, 200 μm. **(B)** mRNA expression of PLCG1 in Kasumi-1 cells after knockout of CREB (left panel) or FOS (right panel) using CRISPR/Cas9 (gCREB #1 and #2; gFOS #1 and #2) or a non-targeting control (NT). *n*=3 independent experiments, in triplicate; paired *t*-test. **(C)** Western Blot analysis of Kasumi-1 cells on day 7 post-infection with either JUN, CREB1 or FOS gRNAs, respectively, or non-targeting control (gNT). GAPDH was used as a loading control.

Supplemental Figure 5

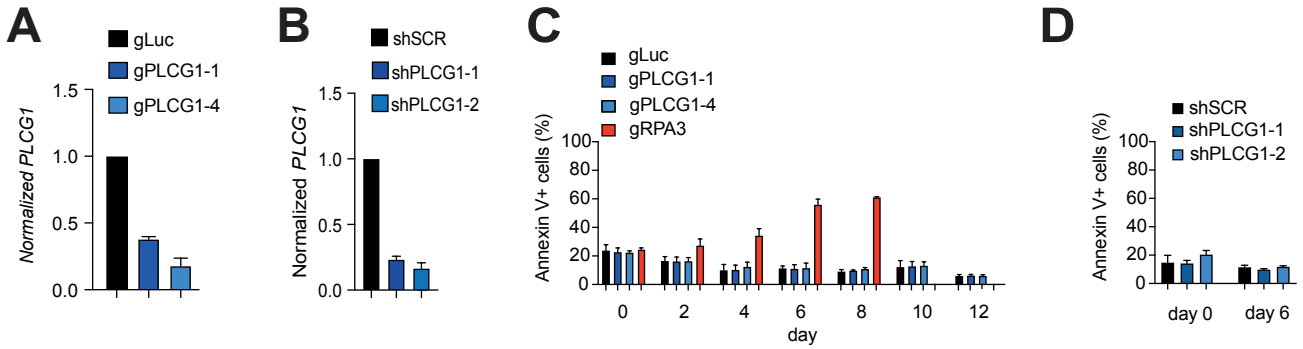

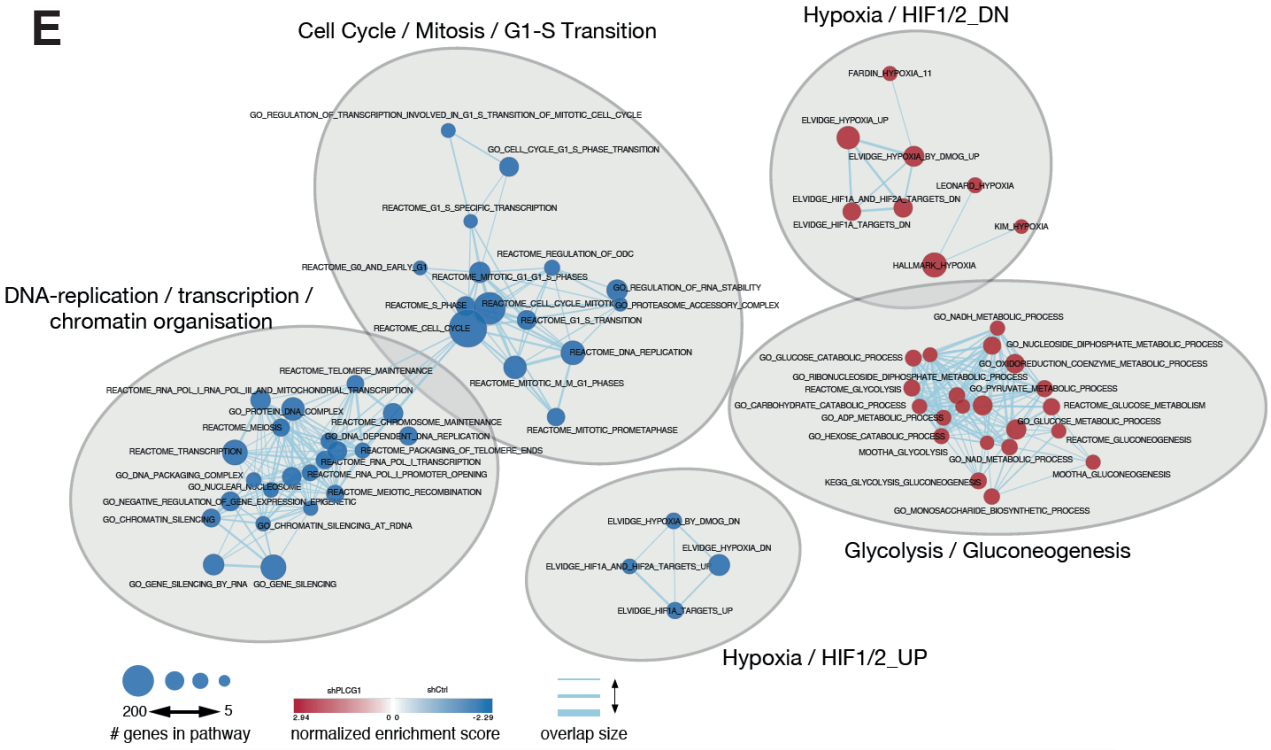

Supplemental Figure 5. AML1-ETO induced cellular functions depend on PLCG1. (A) RT-qPCR in SKNO1_Cas9-Blast cells transduced with sgRNAs targeting PLCG1 or a non-targeting control (gLuc). *n*=3 independent experiments, in triplicate. **(B)** RT-qPCR analysis of PLCG1 mRNA expression in Kasumi-1 cells 5 days after infection with either PLCG1 shRNA (1-1 or 1-2) or non-targeting control (shSCR). *n*=3 independent experiments, in triplicate. **(C)** Apoptosis assay using Annexin V/SYTOX Blue Dead Cell staining in SKNO-1_Cas9-Blast cells infected with gRNAs targeting PLCG1, RPA3 or a non-targeting control (gLuc). *n*=5 independent experiments. **(D)** Apoptosis assay using Annexin V/SYTOX Blue Dead Cell staining in Kasumi-1 cells transduced with shRNAs targeting PLCG1 or a non-targeting control (gSCR). *n*=4 independent experiments. **(E)** PLCG1 knockdown signature tested against more than 10,000 gene sets from MSigDB [6].

Supplemental Figure 6

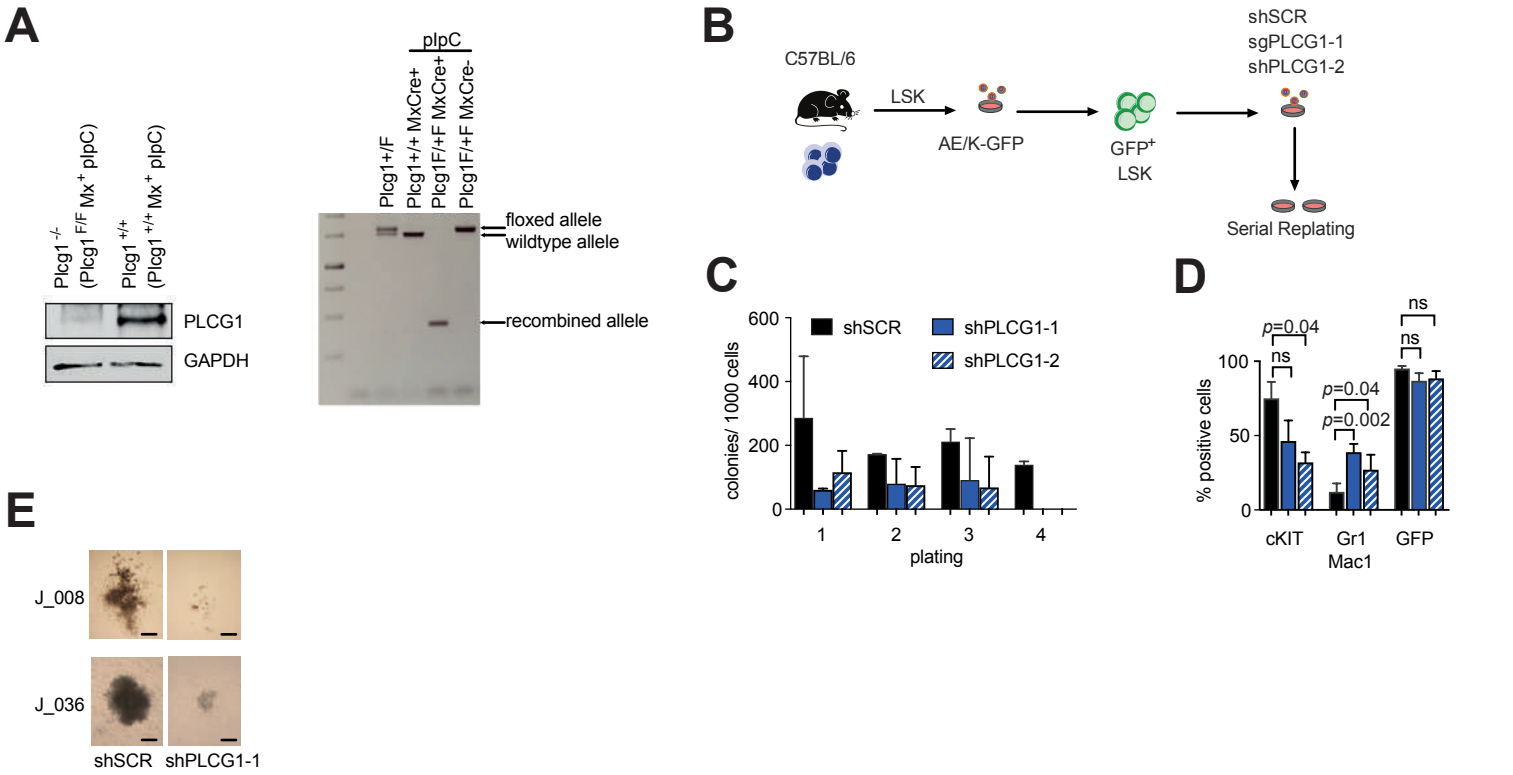

Supplemental Figure 6. AML1-ETO transformed hematopoietic stem cells depend on PLCG1.

(A) Western blot analysis of Plcg1+/+ and Plcg1-/- whole bone marrow cells (left panel) and PCR analysis (right panel) of tail DNA from Plcg1+/F, Plcg1+/+ Mx+, Plcg1F/F Mx+ and Plcg1F/F Cre- mice for detection of wildtype/floxed band and detection of excised band (recombined allele). **(B)** Schematic representation of the experimental set-up to study the effects of *PLCG1* inactivation on AML1-ETO9a (AE)- transformed LSCs *in vitro*. **(C)** Serial replating of AE-transformed LSK cells after genetic inactivation of *Plcg1*. C57BL/6J LSK cells were retrovirally transduced with AE (MSCV-AE-GFP) following genetic depletion of *Plcg1* by RNAi (shPLCG1-1, shPLCG1-2) compared to non-targeting control (shSCR). $1x10^3$ cells were serially plated in methylcellulose. Absolute colony numbers during re-plating over 4 weeks are depicted. *n*=3 independent experiments. **(D)** Immunophenotypic analysis of colonies investigated by flow cytometry. *n*=3 independent experiments; ns=not significant, paired *t*-test. **(E)** Representative pictures of colonies from t(8;21) AML bone marrow cells after after infection with either PLCG1 shRNA (1-1) or non-targeting control (shSCR). Scale bars, 200 μm.

Supplemental Figure 7

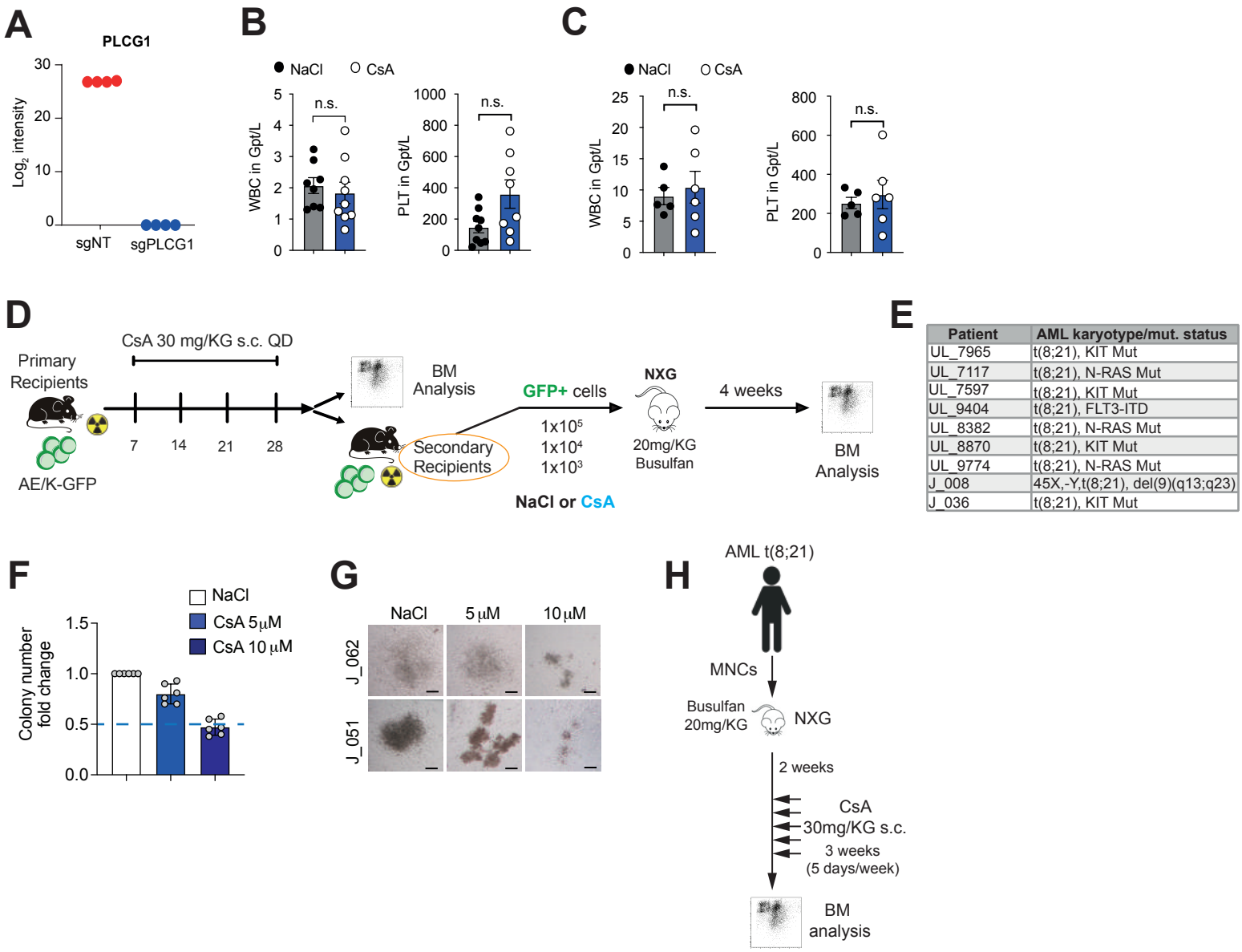

Patient	AML karyotype/mut. status
UL_7965	t(8;21), KIT Mut
UL_7117	t(8;21), N-RAS Mut
UL_7597	t(8;21), KIT Mut
UL_9404	t(8;21), FLT3-ITD
UL_8382	t(8;21), N-RAS Mut
UL_8870	t(8;21), KIT Mut
UL_9774	t(8;21), N-RAS Mut
J_008	45X,-Y,t(8;21), del(9)(q13;q23)
J_036	t(8;21), KIT Mut

Supplemental Figure 7. PLCG1 is required for maintenance of AML1-ETO LSC and pharmacologic suppression of Ca++-signaling inhibits AML1-ETO LSC function. (A) PLCG1 protein expression in SKNO-1_Cas9-Blast cells transduced with sgRNAs targeting PLCG1 or a non-targeting control (sgNT) used for whole proteome analysis. 4 replicates for each condition. **(B)** White blood cell (WBC) count (left panel) and platelet count (right panel) of AE/K primary recipient mice treated with CsA (30mg/kg, s.c., QD) or diluent control (NaCl 0.9%) (n.s.=not significant). **(C)** WBC count (left panel) and platelet count (right panel) of MA9 primary recipient mice treated with CsA (30mg/kg, s.c., QD) or diluent control (NaCl 0.9%) (n.s.=not significant). **(D)** Experimental design of the limiting dilution assay of NaCl- vs. CsA-treated AML1-ETO/KRAS (AE/K) LSC frequency in recipients injected with $1x10^3$, $1x10^4$ or $1x10^5$ viable GFP+ (AE/K) AML cells (n=5 mice per dilution and treatment). **(E)** Molecular analysis of t(8;21) AML patient samples applied for colony forming assays. **(F)** Colony formation of primary human non-AE/non-t(8;21) AML cells (*n*=6 individual patients). Colony number per sample following pharmacologic inhibition with CsA (5, 10 μM) compared to diluent control (NaCl 0.9%). **(G)** Representative pictures of colonies from non-t(8;21) AML bone marrow cells after pharmacological inhibition with cyclosporin A compared to diluent control (NaCl). Scale bars, 200 μm. **(H)** Experimental protocol for investigation on AML engraftment following cyclosporin A (CsA) treatment.

Supplemental references

1. Heidel FH, Bullinger L, Arreba-Tutusaus P, et al. The cell fate determinant Llgl1 influences HSC fitness and prognosis in AML. *J Exp Med*. 2013;210(1):15-22.
2. Huber W, Carey VJ, Gentleman R, et al. Orchestrating high-throughput genomic analysis with Bioconductor. *Nat Methods*. 2015;12(2):115-121.
3. Durinck S, Spellman PT, Birney E, Huber W. Mapping identifiers for the integration of genomic datasets with the R/Bioconductor package biomaRt. *Nat Protoc*. 2009;4(8):1184-1191.
4. Volders PJ, Verheggen K, Menschaert G, et al. An update on LNCipedia: a database for annotated human lncRNA sequences. *Nucleic Acids Res*. 2015;43(Database issue):D174-180.
5. Ritchie ME, Phipson B, Wu D, et al. limma powers differential expression analyses for RNA-sequencing and microarray studies. *Nucleic Acids Res*. 2015;43(7):e47.
6. Subramanian A, Tamayo P, Mootha VK, et al. Gene set enrichment analysis: a knowledge-based approach for interpreting genome-wide expression profiles. *Proc Natl Acad Sci U S A*. 2005;102(43):15545-15550.
7. Schwarzer A, Emmrich S, Schmidt F, et al. The non-coding RNA landscape of human hematopoiesis and leukemia. *Nat Commun*. 2017;8(1):218.
8. Merico D, Isserlin R, Stueker O, Emili A, Bader GD. Enrichment map: a network-based method for gene-set enrichment visualization and interpretation. *PLoS One*. 2010;5(11):e13984.
9. Ptasinska A, Assi SA, Martinez-Soria N, et al. Identification of a dynamic core transcriptional network in t(8;21) AML that regulates differentiation block and self-renewal. *Cell Rep*. 2014;8(6):1974-1988.
10. Ptasinska A, Pickin A, Assi SA, et al. RUNX1-ETO Depletion in t(8;21) AML Leads to C/EBPalpha- and AP-1-Mediated Alterations in Enhancer-Promoter Interaction. *Cell Rep*. 2019;29(7):2120.
11. Martinez-Soria N, McKenzie L, Draper J, et al. The Oncogenic Transcription Factor RUNX1/ETO Corrupts Cell Cycle Regulation to Drive Leukemic Transformation. *Cancer Cell*. 2018;34(4):626-642 e628.
12. Langmead B, Salzberg SL. Fast gapped-read alignment with Bowtie 2. *Nat Methods*. 2012;9(4):357-359.
13. Quinlan AR, Hall IM. BEDTools: a flexible suite of utilities for comparing genomic features. *Bioinformatics*. 2010;26(6):841-842.
14. Kent WJ, Sugnet CW, Furey TS, et al. The human genome browser at UCSC. *Genome Res*. 2002;12(6):996-1006.
15. Zhang Y, Liu T, Meyer CA, et al. Model-based analysis of ChIP-Seq (MACS). *Genome Biol*. 2008;9(9):R137.
16. Ji H, Jiang H, Ma W, Johnson DS, Myers RM, Wong WH. An integrated software system for analyzing ChIP-chip and ChIP-seq data. *Nat Biotechnol*. 2008;26(11):1293-1300.
17. Dobin A, Davis CA, Schlesinger F, et al. STAR: ultrafast universal RNA-seq aligner. *Bioinformatics*. 2013;29(1):15-21.
18. Love MI, Huber W, Anders S. Moderated estimation of fold change and dispersion for RNA-seq data with DESeq2. *Genome Biol*. 2014;15(12):550.
19. Reich M, Liefeld T, Gould J, Lerner J, Tamayo P, Mesirov JP. GenePattern 2.0. *Nat Genet*. 2006;38(5):500-501.
20. Haferlach T, Kohlmann A, Wieczorek L, et al. Clinical utility of microarray-based gene expression profiling in the diagnosis and subclassification of leukemia: report from the International Microarray Innovations in Leukemia Study Group. *J Clin Oncol*. 2010;28(15):2529-2537.
21. Wouters BJ, Lowenberg B, Erpelinck-Verschueren CA, van Putten WL, Valk PJ, Delwel R. Double CEBPA mutations, but not single CEBPA mutations, define a subgroup of acute myeloid leukemia with a distinctive gene expression profile that is uniquely associated with a favorable outcome. *Blood*. 2009;113(13):3088-3091.
22. Stavropoulou V, Kaspar S, Brault L, et al. MLL-AF9 Expression in Hematopoietic Stem Cells Drives a Highly Invasive AML Expressing EMT-Related Genes Linked to Poor Outcome. *Cancer Cell*. 2016;30(1):43-58.
23. Piper J, Elze MC, Cauchy P, Cockerill PN, Bonifer C, Ott S. Wellington: a novel method for the accurate identification of digital genomic footprints from DNase-seq data. *Nucleic Acids Res*. 2013;41(21):e201.
24. Bevington SL, Cauchy P, Piper J, et al. Inducible chromatin priming is associated with the establishment of immunological memory in T cells. *EMBO J*. 2016;35(5):515-535.